

# UVCGAN: UNET VISION TRANSFORMER CYCLE-CONSISTENT GAN FOR UNPAIRED IMAGE-TO-IMAGE TRANSLATION

Dmitrii Torbunov<sup>1</sup>, Yi Huang<sup>2</sup>, Haiwang Yu<sup>1</sup>, Jin Huang<sup>1</sup>,  
Shinjai Yoo<sup>2</sup>, Meifeng Lin<sup>2</sup>, Brett Viren<sup>1</sup>, Yihui Ren<sup>2</sup>

<sup>1</sup>Physics Department, Brookhaven National Laboratory, Upton, NY, USA

<sup>2</sup>Computational Science Initiative, Brookhaven National Laboratory, Upton, NY, USA

## ABSTRACT

Image-to-image translation has broad applications in art, design, and scientific simulations. The original CycleGAN model emphasizes one-to-one mapping via a cycle-consistent loss, while more recent works promote one-to-many mapping to boost diversity of the translated images. With scientific simulation and one-to-one needs in mind, this work examines if equipping CycleGAN with a vision transformer (ViT) and employing advanced generative adversarial network (GAN) training techniques can achieve better performance. The resulting UNet ViT Cycle-consistent GAN (UVCGAN) model is compared with previous best-performing models on open benchmark image-to-image translation datasets, Selfie2Anime and CelebA. UVCGAN performs better and retains a strong correlation between the original and translated images. An accompanying ablation study shows that the gradient penalty and BERT-like pre-training also contribute to the improvement. To promote reproducibility and open science, the source code, hyperparameter configurations, and pre-trained model will be made available at: <https://github.com/LS4GAN/uvcgan>.

**Index Terms**—Generative Adversarial Networks, Vision Transformer, Unpaired Image-to-image Translation, Self-supervised Pre-training, UNet

## 1. INTRODUCTION

Unpaired image-to-image translation maps images between two or more domains, where image instances are not matched. Gathering datasets with exact pixel-to-pixel mapping is difficult and often impossible as most of scientific experiments cannot be exactly reproduced by simulations. Differing from regular generative models [1, 2, 3] that create images from random vector inputs, image-to-image translation derives from an input image, which hypothetically should be an

---

This work was supported by the Laboratory Directed Research and Development Program of Brookhaven National Laboratory, which is operated and managed for the U.S. Department of Energy Office of Science by Brookhaven Science Associates under contract No. DE-SC0012704.

easier task. Along with its potential applications in art and design, we believe image-to-image translation will have a profound impact in scientific simulations [4]. Instead of replacing an entire scientific simulation with a generative model, simulation results could be defined as one domain with experimental data as the other. Thus, an image-to-image translation model would fill the simulation-reality gap.

The CycleGAN [5, 6, 7] model connects two generative adversarial network (GAN) models, one for each translation direction, and introduces a cycle-consistent loss that reinforces an image should look like itself after a cycle translation, i.e., translated to the other domain and back. Other methods [8, 9, 10, 11, 12] promote the translation diversity or one-to-many mapping between two domains. More recently, ACL-GAN [11] relaxes the self-consistent constraint by introducing a so-called “adversarial-consistency loss,” a self-consistency loss at the distribution level. Council-GAN [10] completely discards the idea of self-consistency, employs an ensemble of generators, and only works in one translation direction. To boost diversity, both models have injected random noise into the feature space. Although these models have shown promising improvement on benchmark data, features like stochasticity and diversity are not desirable for many scientific applications. The question is: *can newer deep learning architectures and techniques improve the one-to-one deterministic translation with cycle-consistent loss?*

Convolutional neural network (CNN) architecture has been a popular choice for computer vision tasks. In the natural language processing (NLP) field, the attention mechanism and transformer-style architecture have surpassed previous models, such as hidden Markov models and recurrent neural networks in open benchmark tasks. Compared to CNNs, transformers can capture long-distance patterns, which are common in nature. Applications of transformers in computer vision have debuted in [13], while other recent work has shown that a CNN-transformer hybrid can achieve better performance [14, 15]. In this work, we will examine how much improvement transformer and GAN training techniques can bring to the classic CycleGAN.

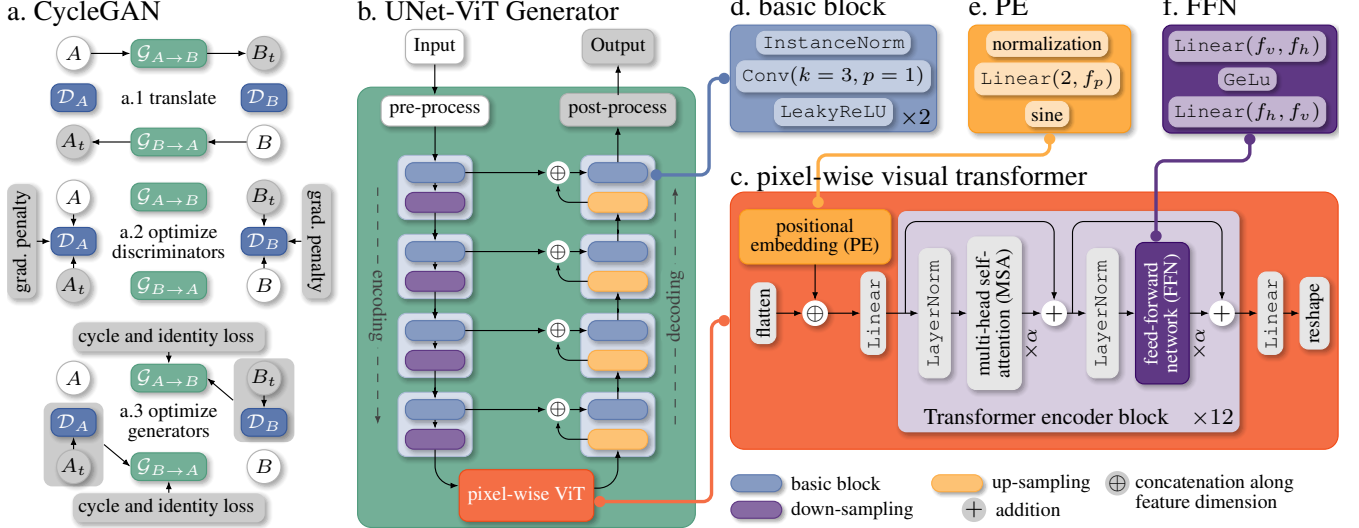


**Fig. 1. Schematic diagrams of UVCGAN:** a) CycleGAN, b) UNet-ViT generator, and c) pixel-wise ViT.

## 2. METHOD

### 2.1. Proposed Network Architecture: UVCGAN

**CycleGAN-like models** [5, 6, 7] interlace two generator-discriminator pairs for unpaired image-to-image translation. Let us denote two image domains,  $A$  and  $B$ . A typical CycleGAN-like model has two generators:  $\mathcal{G}_{A \rightarrow B}$  that translates images from  $A$  to  $B$  and  $\mathcal{G}_{B \rightarrow A}$  that translates from  $B$  to  $A$  (Fig. 1a.1). It also has two discriminators:  $\mathcal{D}_A$  that distinguishes between images in  $A$  and those translated from  $B$ , and  $\mathcal{D}_B$  that differentiates images in  $B$  and those translated from  $A$ .

The **UNet-ViT generator** consists of a UNet [16] with a pixel-wise ViT (vision transformer) [17] at the bottleneck (Fig. 1b). UNet’s encoding path extracts features at every basic block (Fig. 1d) by reducing spatial dimensions and enriching the feature dimension then passes these features to the decoding path. In turn, the decoding path converts features to images. Passing the pre-process layer, the image becomes a tensor with dimensions of  $(w_0, h_0, f_0)$ , and the encoding path maps it into  $(w, h, f)$ , where  $w = w_0/16$ ,  $h = h_0/16$ , and  $f = 8f_0$ . At every basic block in the encoding path, the width and height dimensions are halved, and the feature dimension is doubled—except the first one (Fig. 1b). Similarly, the decoding path processes the output from pixel-wise ViT through a sequence of up-sampling and `conv` layers. Each basic block doubles the width and height and halves the feature dimension. The pre-process layer consists of a `conv` and leaky ReLU (rectified linear unit), whereas the post-process layer is  $1 \times 1$ -`conv` and sigmoid.

A **pixel-wise ViT** bridges the end of the encoding path and start of the UNet decoding path (Fig. 1c). The ViT initially flattens the spacial dimensions to get a feature matrix of di-

mension  $(w \times h, f)$  then concatenates it with a Fourier positional embedding [18] (Fig. 1e), resulting in a feature matrix of dimension  $(w \times h, f + f_p)$  followed by a linear layer mapping  $f + f_p$  to  $f_v$ . A multi-head self-attention transformer consists of a stack of twelve encoder blocks. Diverging from the original encoder block design [19], we adopt the rezero regularization [20] by introducing a trainable scaling parameter  $\alpha$ . Before passing the output to the decoding path, ViT reshapes it to restore its spatial dimensions. In our study, the feature dimension  $f, f_p, f_v = 384$ , and the linear expansion dimension  $f_h = 4f_v$  (Fig. 1f).

### 2.2. Pre-training and Loss Function

**Bidirectional Encoder Representations from Transformers (BERT)-like self-supervised pre-training** is an effective way to prime large randomly initialized networks for downstream tasks [21, 22]. The models are trained to predict the original unmasked images from the masked ones using a pixel-wise  $\ell_1$  loss function. This poses an intriguing question: is a smaller yet similar dataset or a large, diverse one more suitable for pre-training? To assess the former, we use the same dataset as the downstream image translation task for pre-training. For the latter, the ImageNet [23] is used. We initialize both CycleGAN generators from the same pre-trained model.

$$\mathcal{L}_{\text{gen}} = \mathcal{L}_{\text{GAN}} + \lambda_{\text{idt}} \mathcal{L}_{\text{idt}} + \lambda_{\text{cyc}} \mathcal{L}_{\text{cyc}} \quad (1)$$

$$\mathcal{L}_{\text{disc}} = -\mathcal{L}_{\text{GAN}} + \lambda_{\text{GP}} \mathbb{E}_x \left[ (\|\nabla_x \mathcal{D}(x)\|_2 - \gamma)^2 / \gamma^2 \right] \quad (2)$$

**Loss Function with Gradient Penalty (GP).** The original generator loss function [5] is a linear combination of three

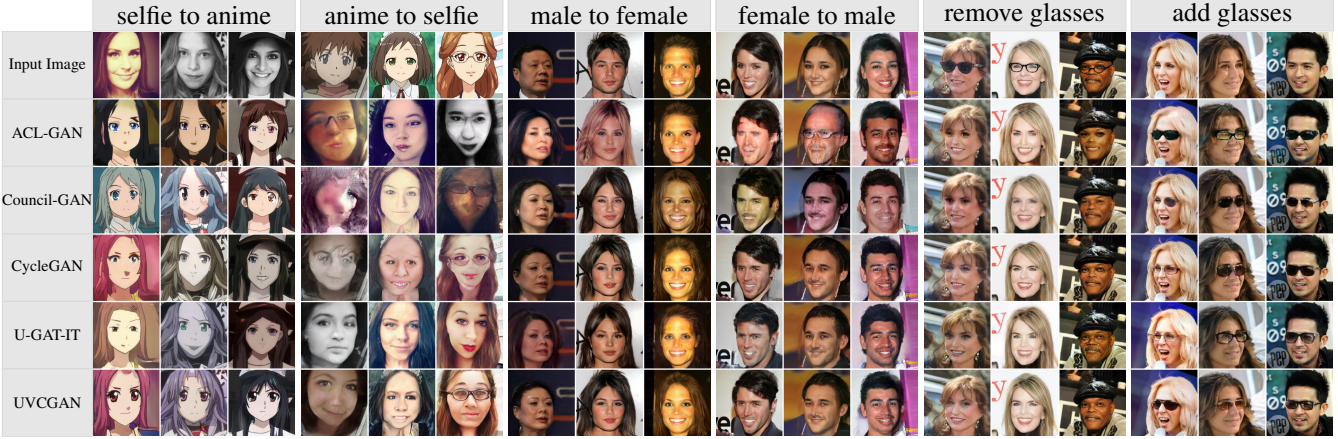


**Fig. 2.** Translated image samples.

parts (Eq. (1)), where  $\mathcal{L}_{\text{GAN}}$  is an adversarial loss,  $\mathcal{L}_{\text{idt}}$  is an identity loss, and  $\mathcal{L}_{\text{cyc}}$  is a cycle-consistency loss.  $\lambda_{\text{idt}}$  and  $\lambda_{\text{cyc}}$  are the corresponding scaling hyperparameters. To improve GAN training stability, we replace the  $\mathcal{L}_{\text{GAN}}$  with a least square (LS) GAN loss [24] and add a gradient penalty [25, 26] to the discriminator loss (Eq. (2)). We use a form of the gradient penalty term suggested by [27] with adjustable  $\lambda_{\text{GP}}$  and  $\gamma$  hyperparameters. Training CycleGAN involves a traditional two-step minimax game [1], where the discriminator attempts to minimize  $\mathcal{L}_{\text{disc}}$  (Fig. 1.1a.2) and the generator tries to minimize  $\mathcal{L}_{\text{gen}}$  (Fig. 1.1a.3).

### 3. EXPERIMENTS AND RESULTS

#### 3.1. Evaluation Datasets

We select three popular and challenging unpaired image-to-image translation benchmark tasks: selfie $\leftrightarrow$ anime [12], male $\leftrightarrow$ female, and adding/removing glasses, following the most recent developments [11, 12, 10, 28, 29, 30]. Both male $\leftrightarrow$ female and adding/removing glasses tasks are derived from the CelebA [31] based on the gender attribute and wearing glasses. Selfie2Anime is relatively small but balanced with 3.4K images in each domain, while male $\leftrightarrow$ female is large with about 68K males and 95K females. The adding/removing glasses benchmark is imbalanced as there are 11K with glasses and 152K without. To achieve a fair comparison, we do not use CelebA’s validation dataset for training. Instead, we combine it with the test dataset following the convention of [10, 11].

#### 3.2. Training Details

**BERT-like generator pre-training** is a self-supervised approach to task the generator with restoring impaired images. To construct BERT-like tokens, images of size  $256 \times 256$  are tiled into  $32 \times 32$  pixel patches, and patches are masked with

a probability of 40% by zeroing their pixel values. We use the Adam optimizer; cosine annealing learning-rate scheduler; and several standard data augmentations, such as small-angle random rotation, random cropping, random flipping, and color jittering. During pre-training, we do not distinguish the image domains. Therefore, for all downstream tasks, we only pre-train three generators, one for each dataset: ImageNet, CelebA, and Selfie2Anime.

**UVCGAN image-to-image translation** downstream tasks are trained for  $10^6$  iterations in total using the Adam optimizer with a learning rate of  $10^{-4}$  and a batch size of 1, which is linearly annealed to zero during the second half. We apply three data augmentations: resizing, random cropping, and random horizontal flipping. Before random cropping images to  $256 \times 256$ , we enlarge them from  $256 \times 256$  to  $286 \times 286$  for Selfie2Anime and  $178 \times 218$  to  $256 \times 313$  for CelebA.

**Hyperparameter search** is done via a small-scale grid search to discover the best-performing hyperparameter configurations. Our experiments show the best performance is achieved when the UVCGAN is trained with the LSGAN-GP ( $\lambda_{\text{GP}} = 0.1, \gamma = 100$ ) loss function, and the generator is pre-trained on the same dataset where the downstream image translation is performed. Optimal  $\lambda_{\text{cyc}}$  differs slightly for CelebA and Selfie2Anime, 5 and 10, respectively, and  $\lambda_{\text{idt}}$  is kept at half of  $\lambda_{\text{cyc}}$ . While we also tried Wasserstein-GAN GP loss, it is more sensitive to hyperparameters and yields overall worse results. The effectiveness of combining LSGAN with GP echoes the finding in [26]. More training details can be found in the open-source repository [32].

#### 3.3. Evaluation Results

Fréchet Inception Distance (FID) [33] and Kernel Inception distance (KID) [34] are the two most accepted metrics for evaluating image-to-image translation performance. A lower distance score means the translated images are more similar

**Table 1. FID and KID scores.** Lower is better.

	selfie to anime				anime to selfie				male to female		female to male		remove glasses		add glasses	
	FID	KID ( $\times 100$ )	FID	KID ( $\times 100$ )	FID	KID ( $\times 100$ )	FID	KID ( $\times 100$ )	FID	KID ( $\times 100$ )	FID	KID ( $\times 100$ )	FID	KID ( $\times 100$ )	FID	KID ( $\times 100$ )
ACL-GAN [11]	99.3	$3.22 \pm 0.26$	128.6	$3.49 \pm 0.33$	<b>9.4</b>	<b><math>0.58 \pm 0.06</math></b>	19.1	$1.38 \pm 0.09$	16.7	$0.70 \pm 0.06$	26.6	$2.26 \pm 0.17$				
Council-GAN [10]	91.9	$2.74 \pm 0.26$	126.0	$2.57 \pm 0.32$	10.4	$0.74 \pm 0.08$	24.1	$1.79 \pm 0.10$	37.2	$3.67 \pm 0.22$	19.5	$1.33 \pm 0.13$				
CycleGAN [5]	93.4	$2.96 \pm 0.27$	129.4	$2.91 \pm 0.39$	15.2	$1.29 \pm 0.11$	22.2	$1.74 \pm 0.11$	24.2	$1.87 \pm 0.17$	19.8	$1.36 \pm 0.12$				
U-GAT-IT [12]	95.8	$2.74 \pm 0.31$	<b>108.8</b>	<b><math>1.48 \pm 0.34</math></b>	12.6	$0.88 \pm 0.08$	23.1	$1.91 \pm 0.12$	20.9	$1.39 \pm 0.13$	20.0	$1.16 \pm 0.09$				
UVCGAN (Ours)	<b>79.0</b>	<b><math>1.35 \pm 0.20</math></b>	122.8	$2.33 \pm 0.38$	9.6	$0.68 \pm 0.07$	<b>13.9</b>	<b><math>0.91 \pm 0.08</math></b>	<b>14.4</b>	<b><math>0.68 \pm 0.10</math></b>	<b>13.6</b>	<b><math>0.60 \pm 0.08</math></b>				

to those in the target domain. As shown in Table 1, our model offers better performance in most image-to-image translation tasks compared to existing models. As a cycle-consistent model, our model’s translated images correlate strongly with the input images, such as hair color and face orientations (Fig. 2), which is crucial for augmenting scientific simulations. **Remark:** KID and FID for image-to-image translation are difficult to reproduce. In [10, 11, 12], most FID and KID scores of the same task-model settings differ. We hypothesize that this is due to: 1) different sample sizes of test data as FID will decrease with more data samples [34], 2) the differences in post-processing before testing, and 3) the use of different FID and KID implementations. Therefore, we employ the full test dataset for FID, and 50 (Selfie2Anime) and 1000 (CelebA) subset size for KID. For non-square CelebA images, we first resize them to have a central crop of size  $256 \times 256$ , so a face has the same aspect ratio. All calculations of KID and FID are delegated to the open-source torch-fidelity package [35]. To faithfully reproduce existing models, we use pre-trained models (if available). Otherwise, we retrain them following the provided hyperparameter configurations. To help evaluate and reproduce our results, there are more details about pre-trained models, training and evaluation procedures, and additional sample images in [32].

### 3.4. Ablation Study

Here, we analyze the influence of various design decisions and hyperparameter configurations on the UVCGAN model’s performance, specifically how various pre-training datasets affect the performance, e.g., will using a large, diverse ImageNet perform better than a smaller, task-relevant CelebA or Selfie2Anime? Table 2 summarizes the male-to-female and selfie-to-anime translation performance with respect to using different pre-training datasets (“None” when no pre-training is used), GP loss ( $\mathcal{L}_{GP}$ ), and identity loss ( $\mathcal{L}_{idt}$ ). Table 2 details numerous observations. First, GP combined with identity loss improves the performance. Second, without GP, the identity loss produces mixed results. Finally, pre-training on the same dataset improves the performance, especially in conjunction with the GP and identity loss.

We speculate that the reason why the GP is required for obtaining the best performance with pre-trained networks is because those networks provide a good starting point for the

**Table 2. Ablation studies.** Pretrain/Dataset column indicates which dataset the generator is pre-trained on (*None* for no pre-training; *Same* indicates CelebA for male-to-female and Selfi2Anime for selfie-to-anime).

Pretrain Dataset	male to female				selfie to anime	
	$\mathcal{L}_{GP}$	$\mathcal{L}_{idt}$	FID	KID ( $\times 100$ )	FID	KID ( $\times 100$ )
Same	✓	✓	9.6	$0.68 \pm 0.07$	79.0	$1.35 \pm 0.20$
ImageNet	✓	✓	11.0	$0.85 \pm 0.08$	81.3	$1.66 \pm 0.21$
None	✓	✓	11.0	$0.85 \pm 0.09$	80.9	$1.78 \pm 0.20$
Same	✓		11.1	$0.86 \pm 0.08$	83.9	$1.88 \pm 0.35$
ImageNet	✓		11.0	$0.85 \pm 0.08$	84.3	$1.77 \pm 0.21$
None	✓		13.4	$1.11 \pm 0.09$	115.4	$6.85 \pm 0.59$
Same		✓	14.2	$1.22 \pm 0.10$	81.5	$1.68 \pm 0.22$
ImageNet		✓	14.5	$1.23 \pm 0.10$	86.8	$2.21 \pm 0.25$
None		✓	14.4	$1.26 \pm 0.10$	81.6	$1.75 \pm 0.25$
Same			12.7	$1.06 \pm 0.09$	79.0	$1.32 \pm 0.19$
ImageNet			13.4	$1.14 \pm 0.10$	91.2	$2.63 \pm 0.23$
None			18.3	$1.63 \pm 0.11$	81.2	$1.76 \pm 0.21$

image translation task. However, right at the beginning of fine-tuning, the discriminator is initialized by random values and provides a meaningless signal to the generator. This random signal may drive the generator away from the good starting point and undermine the benefit of pre-training. If this is true, perhaps pre-training the discriminator will further improve our results.

## 4. CONCLUSION

This work introduces UVCGAN to promote cycle-consistent content-preserving image translation and effectively handle long-range spatial dependencies that remain a common problem in scientific domain research. Combined with BERT-like self-supervised pre-training and the GP regularization, UVCGAN outperforms other advanced algorithms on a diverse set of image translation benchmarks. The ablation study suggests gradient penalty and cycle-consistent loss work well with UVCGAN. To further demonstrate the effectiveness of ViT handling long-distance patterns in image-to-image translation tasks, we believe openly available scientific datasets are needed.

## 5. REFERENCES

- [1] Ian Goodfellow, Jean Pouget-Abadie, et al., “Generative adversarial nets,” *Advances in neural information processing systems*, vol. 27, 2014.
- [2] Andrew Brock, Jeff Donahue, et al., “Large scale gan training for high fidelity natural image synthesis,” *arXiv preprint arXiv:1809.11096*, 2018.
- [3] Tero Karras, Samuli Laine, et al., “Analyzing and improving the image quality of stylegan,” in *Proceedings of the IEEE/CVF conference on computer vision and pattern recognition*, 2020, pp. 8110–8119.
- [4] Kyle Cranmer, Johann Brehmer, et al., “The frontier of simulation-based inference,” *Proceedings of the National Academy of Sciences*, vol. 117, no. 48, pp. 30055–30062, 2020, Publisher: National Academy of Sciences Section: Colloquium Paper.
- [5] Jun-Yan Zhu, Taesung Park, et al., “Unpaired image-to-image translation using cycle-consistent adversarial networks,” in *2017 IEEE International Conference on Computer Vision (ICCV)*, 2017, pp. 2242–2251, ISSN: 2380-7504.
- [6] Taeksoo Kim, Moonsu Cha, et al., “Learning to discover cross-domain relations with generative adversarial networks,” in *Proceedings of the 34th International Conference on Machine Learning - Volume 70*. 2017, ICML’17, pp. 1857–1865, JMLR.org.
- [7] Zili Yi, Hao Zhang, et al., “Dualgan: Unsupervised dual learning for image-to-image translation,” in *Proceedings of the IEEE international conference on computer vision*, 2017, pp. 2849–2857.
- [8] Xun Huang, Ming-Yu Liu, et al., “Multimodal unsupervised image-to-image translation,” in *Proceedings of the European conference on computer vision (ECCV)*, 2018, pp. 172–189.
- [9] Hsin-Ying Lee, Hung-Yu Tseng, et al., “Diverse image-to-image translation via disentangled representations,” in *Proceedings of the European conference on computer vision (ECCV)*, 2018, pp. 35–51.
- [10] Ori Nizan and Ayellet Tal, “Breaking the cycle–colleagues are all you need,” in *2020 IEEE/CVF Conference on Computer Vision and Pattern Recognition (CVPR)*. IEEE, 2020, pp. 7857–7866.
- [11] Yihao Zhao, Ruihai Wu, et al., “Unpaired image-to-image translation using adversarial consistency loss,” in *European Conference on Computer Vision*. Springer, 2020, pp. 800–815.
- [12] Junho Kim, Minjae Kim, et al., “U-gat-it: Unsupervised generative attentional networks with adaptive layer-instance normalization for image-to-image translation,” in *International Conference on Learning Representations*, 2019.
- [13] Alexey Dosovitskiy, Lucas Beyer, et al., “An image is worth 16x16 words: Transformers for image recognition at scale,” *arXiv preprint arXiv:2010.11929*, 2020.
- [14] Tete Xiao, Piotr Dollar, et al., “Early convolutions help transformers see better,” *Advances in Neural Information Processing Systems*, vol. 34, 2021.
- [15] Jianyuan Guo, Kai Han, et al., “Cmt: Convolutional neural networks meet vision transformers,” *arXiv preprint arXiv:2107.06263*, 2021.
- [16] Olaf Ronneberger, Philipp Fischer, et al., “U-net: Convolutional networks for biomedical image segmentation,” in *International Conference on Medical image computing and computer-assisted intervention*. Springer, 2015, pp. 234–241.
- [17] Alexey Dosovitskiy, Lucas Beyer, et al., “An image is worth 16x16 words: Transformers for image recognition at scale,” *arXiv preprint arXiv:2010.11929*, 2020.
- [18] Ivan Anokhin, Kirill Demochkin, et al., “Image generators with conditionally-independent pixel synthesis,” in *Proceedings of the IEEE/CVF Conference on Computer Vision and Pattern Recognition*, 2021, pp. 14278–14287.
- [19] Ashish Vaswani, Noam Shazeer, et al., “Attention is all you need,” in *Advances in neural information processing systems*, 2017, pp. 5998–6008.
- [20] Thomas Bachlechner, Bodhisattwa Prasad Majumder, et al., “Rezero is all you need: Fast convergence at large depth,” in *Uncertainty in Artificial Intelligence*. PMLR, 2021, pp. 1352–1361.
- [21] Jacob Devlin, Ming-Wei Chang, et al., “Bert: Pre-training of deep bidirectional transformers for language understanding,” 2019.
- [22] Hangbo Bao, Li Dong, et al., “Beit: Bert pre-training of image transformers,” *arXiv preprint arXiv:2106.08254*, 2021.
- [23] Jia Deng, Wei Dong, et al., “Imagenet: A large-scale hierarchical image database,” in *2009 IEEE Conference on Computer Vision and Pattern Recognition*, 2009, pp. 248–255.
- [24] Xudong Mao, Qing Li, et al., “Least squares generative adversarial networks,” in *Proceedings of the IEEE international conference on computer vision*, 2017, pp. 2794–2802.
- [25] Ishaa Gulrajani, Faruk Ahmed, et al., “Improved training of wasserstein gans,” 2017.
- [26] Xudong Mao, Qing Li, et al., “On the effectiveness of least squares generative adversarial networks,” *IEEE Transactions on Pattern Analysis and Machine Intelligence*, vol. 41, no. 12, pp. 2947–2960, 2019.
- [27] Tero Karras, Timo Aila, et al., “Progressive growing of gans for improved quality, stability, and variation,” 2018.
- [28] Taesung Park, Alexei A Efros, et al., “Contrastive learning for unpaired image-to-image translation,” in *European Conference on Computer Vision*. Springer, 2020, pp. 319–345.
- [29] Yang Zhao and Changyou Chen, “Unpaired image-to-image translation via latent energy transport,” in *Proceedings of the IEEE/CVF Conference on Computer Vision and Pattern Recognition*, 2021, pp. 16418–16427.
- [30] Hao Tang, Hong Liu, et al., “Attentiongan: Unpaired image-to-image translation using attention-guided generative adversarial networks,” *IEEE Transactions on Neural Networks and Learning Systems*, 2021.
- [31] Ziwei Liu, Ping Luo, et al., “Deep learning face attributes in the wild,” in *Proceedings of International Conference on Computer Vision (ICCV)*, December 2015.
- [32] Dmitrii Torbunov, Yi Huang, et al., “Uvcgan,” <https://github.com/LS4GAN/uvcgan>, 2022.
- [33] Martin Heusel, Hubert Ramsauer, et al., “Gans trained by a two time-scale update rule converge to a local nash equilibrium,” in *Advances in Neural Information Processing Systems*, I. Guyon, U. V. Luxburg, S. Bengio, H. Wallach, R. Fergus, S. Vishwanathan, and R. Garnett, Eds. 2017, vol. 30, Curran Associates, Inc.
- [34] Mikołaj Bińkowski, Danica J Sutherland, et al., “Demystifying mmd gans,” *arXiv preprint arXiv:1801.01401*, 2018.
- [35] Anton Obukhov, Maximilian Seitzer, et al., “High-fidelity performance metrics for generative models in pytorch,” 2020, Version: 0.3.0, DOI: 10.5281/zenodo.4957738.